Chemical Hot Gas cleaning of Alkali, Chlorine, and Sulphur Species in a Sorption Enhanced Gasification Process at 650 °C

Markus Kopsch [a, 1], Patrick Schuster [a], Elena Yazhenskikh [a], Jürgen Sitzmann [b], Michael Müller [a]

[a] Institute of Energy Materials and Devices (IMD-1), Wilhelm-Johnen Straße, 52428 Jülich, Forschungszentrum Jülich GmbH, Germany

[b] Calida Cleantech GmbH, Adlerstraße 2, 91560, Heilsbronn, Germany

Abstract:

The European GICO-Project aimed to develop an advanced approach to convert energy from biomass into biofuel and on-demand power production. In the GICO-Process, a H_2-rich hot gas stream of a gasifier operating at 650 °C has to be cleaned from inorganic contaminants, e.g. H_2S, HCl, and KCl, to protect downstream equipment, e.g. membranes, SOFC and a plasma reactor from corrosion. The use of CaO as a primary sorption material in the gasification reactor reduces the CO_2 amount by forming $CaCO_3$. Moreover, CaO reduces the H_2S and HCl concentration in the gasifier by forming CaS, respectively $CaCl_2$. However, previous studies have shown that these reactions are not sufficient to reduce the H_2S and HCl concentrations below the demanded 1 ppm_v goal. Thus, secondary hot gas cleaning is necessary. As standard sorbents are only used at temperatures up to 600 °C, further consideration of new sorbents developed and investigated in this work is of particular interest.

Thermodynamic model calculations and sorption experiments in lab-scale furnaces were conducted to determine if chemical hot gas cleaning concepts can effectively remove sour gas and alkali components from the syngas leaving a gasification unit operating at 650 °C. In contrast to other studies, gases such as CO_2, H_2O, H_2, and CO were not substituted in the sorption experiments. This realistic gas composition

[1] Corresponding author: m.kopsch@fz-juelich.de (Markus Kopsch)

represents a novel approach at 650 °C, allowing for more representative and reliable experimental results. Using a mass spectrometer, it was possible to record the H_2, CO_2, H_2S, and HCl concentrations during the sorption experiments simultaneously, although the input concentrations of the gas components (H_2: 72 vol-%, CO_2: 1 vol-%, H_2S: 60 ppm_v and HCl: 40 ppm_v) were differing strongly. Zinc titanate, as a conventional sulfur sorbent, reduced the H_2S concentration in the experiments to around 7 ppm_v. Ba-, Sr-, and Ce-containing sorbents achieved H_2S concentrations below 1 ppm_v for several hours, which should be sufficient to prevent poisoning of the nickel catalyst. 6 aluminosilicates, i.e. Bauxite, Clinoptilolite, Kaolin, Bentonite, Montmorillonite, and Cat litter, have been proven to be suitable for KCl reduction to values below 1 ppm_v.

Key Words: Hot Gas Conditiong (HGC), Sorption, Sorption Enhanced Gasification (SEG)

1 Introduction

Although gasification of biomass is technically advanced and has been implemented on a large scale several times, one of the main existing challenges is the development of a resource-saving and cost-effective hot gas conditioning (HGC) system to produce highly pure synthesis gas [1–3]. Impurities contained in syngas include particulates, tars, and inorganics, posing environmental risks. HGC can be used to reduce organic (e.g. tars) and inorganic contaminants (e.g. sulfur, chlorine, alkali metals) released from low-cost fuels during gasification. H_2S, KCl, and HCl are the main contaminants produced during biomass gasification [4, 5]. Moreover, there is a huge difference in terms of contaminant concentration ranging from a few ppm_v to over 1000 ppm_v depending on the biomass.

The EU project GICO ("Gasification Integrated with CO_2 capture and conversion") [6] focused on the development of small to medium scale residual biomass plants based on sorption enhanced gasification. The use of CaO sorbents in a low-temperature-fluidised-bed-gasifier operating at 650 °C shifts the thermodynamic equilibrium towards higher H_2 concentrations (from approximately 40% H_2 to 75% H_2)

which is beneficial for the operation of a high temperature fuel cell. Simultaneously, a CO_2-rich gas stream is produced by calcination of the resulting calcium carbonate at 920 °C allowing for carbon capture and utilization. In this process, two hot gas streams need to be purified to protect downstream equipment like membranes, fuel cells, and plasma reactors.

In the GICO-process, different sulfur compounds are present in gases in different operating units, with SO_2 predominating in calciner gases and H_2S being a by-product of gasification. However, small quantities of each product can be found in either unit. Consequently, it is important to distinguish between HGC methods that remove SO_2 from calciner gases and those that remove H_2S from the gasifier gases. Since H_2S is one of the most problematic sulfur contaminants under gasification conditions, its removal is necessary. However, currently used techniques like wet scrubbing are producing by-products that need to be further treated. Moreover, they are energy intense due to the thermal management (cooling and heating steps) of the feed stream.

Therefore, investigations on chemical HGC were conducted and showed that metal oxides are suitable for sulfur reduction [7–9]. Several Mn-, Ca-, Cu-, Fe-, and Zn-based sorbents with high sulfur capacity have been developed in the temperature range up to 600 °C [10]. It is possible to achieve H_2S concentrations of 1-5 ppm_v for Cu-based sorbents to 10 ppm_v for zinc ferrites in gasifier-derived gases [9, 11]. Although reaction 1 shows that the sorption reaction is sensitive to water, many syngases used for H_2S sorption investigations were only balanced with N_2 or He [12–18].

$$MO_{(s)} + H_2S_{(g)} \leftrightarrow MS_{(s)} + H_2O_{(g)} \quad (1)$$

In order to fulfill the requirement of a nickel catalyst for 1 ppm_v H_2S in the high temperature range of 800-900 °C, investigations were carried out with barium-based sorbents. Thermodynamic calculations indicated that stabilized Ba sorbents should retain 1 ppm_v H_2S, therefore the stabilization of the sorbent by CaO was investigated [19].

CaO-BaO shows low solubility at temperatures above 1200 °C. Therefore, in previous studies a sorbent was prepared from a mixture of BaO and CaO. The sorbent reduced the H_2S concentrations to values below 0.5 ppm_v in the temperature range of 800-900 °C. The XRD analysis confirmed the stabilization effect by the appearance of a BaS phase in the sorbent, which should normally be unstable under these conditions. At temperatures below 760 °C, the remaining H_2S concentration increased strongly due to the carbonization of the sorbent [10].

Another potential second-generation sorbent for high-temperature gas desulfurization that has been studied is cerium oxide. Reversible adsorption of H_2S on cerium oxide surfaces has been demonstrated over many cycles at temperatures as high as 800 °C [20, 21]. Despite the fact that CeO_2 will react with H_2S, the reaction thermodynamics do not allow H_2S target levels of about 20 ppm_v to be achieved. CeO_2 is reduced at high temperatures to a nonstoichiometric oxide, CeO_n ($n < 2$), which is superior to CeO_2 in removing H_2S. As a function of temperature, pressure, feed gas composition, and flow rate, the reduction and sulfidation reactions were studied in fixed-bed reactors.

Ce_2O_3 forms an oxysulfide with H_2S, but also Ce_2S_3 (see reactions 2-5). The H_2S vapor pressure over Ce_2S_3 is greater than the vapor pressure of H_2S over Ce_2O_2S.

$$2CeO_{2(s)} + H_{2(g)} \rightarrow Ce_2O_{3(s)} + H_2O_{(g)} \quad (2)$$

$$2CeO_{2(s)} + H_2S_{(g)} + H_{2(g)} \rightarrow Ce_2O_2S_{(s)} + 2\,H_2O_{(g)} \quad (3)$$

$$Ce_2O_{3(s)} + H_2S_{(g)} \rightarrow Ce_2O_2S_{(s)} + H_2O_{(g)} \quad (4)$$

$$Ce_2O_{3(s)} + 3H_2S_{(g)} \rightarrow Ce_2S_{3(s)} + 3\,H_2O_{(g)} \quad (5)$$

It has been shown that it is marginally more effective to produce CeO_n as a separate step before reduction rather than simultaneously combined reduction and sulfidation. Despite this, both approaches were able to reduce H_2S below the levels of 20 ppm_v [20]. Table 1 summarizes the estimated tolerance limits for H_2S that are expected to severely affect solid oxide fuel cells (SOFC) performance.

Table 1: Tolerance limits of inorganic contaminants for SOFC [22, 23]

Contaminant	Concentration [ppm_v]
H_2S	1-3
HCl	10-200
Alkali	10-200

However, lower concentrations of detrimental inorganic species in the syngas can not only be achieved by gas purification but also by impurity retention. Additives, such as lime, dolomite, or kaolin to reduce the release of sulfur and alkali species can be added to the fuel [24, 25]. In conventional direct combustion processes, the most common technology to reduce sulfur at high temperature revolves around pulverizing $CaCO_3$ or dolomite, which is then fed into the combustion chamber. This means that SO_2 is removed right after combustion, before any gaseous material is produced. In general, it can be concluded that at higher

98 temperatures (approximately 800 °C) $CaSO_4$ will be produced (reaction 6), while at lower temperatures, in
99 the 450–800 °C region, the solid products are CaS and $CaSO_3$ (reaction 7) as well as $CaSO_4$ [9].

$$CaO_{(s)} + SO_{2(g)} + 0.5O_{2(g)} \rightarrow CaSO_{4(s)} \quad (6)$$

$$CaCO_{3(s)} + SO_{2(g)} \rightarrow CaSO_{3(s)} + CO_{2(g)} \quad (7)$$

100 $CaSO_4$ has a molar volume three times greater than CaO. Therefore, the molar volume of $CaSO_4$ produced
101 during sulfidation will exceed the molar volume of CaO consumed, resulting in an increase in the amount
102 of pore blockage that gradually eliminates SO_2 access to the active surface of CaO [9].
103 Alkali sorption experiments on aluminosilicates (bauxite, bentonite, kaolinite, etc.) have been undertaken
104 in various temperature ranges over the past few decades [26, 27]. Concentrations of a few hundred ppb_v
105 were achieved for several hours at 800 °C [10]. However, reaction 8 indicates the necessity of water [28,
106 29]. Without water, the sorption reaction cannot take place.

$$Al_2O_3 \cdot xSiO_{2(s)} + 2AlkCl_{(g)} + H_2O_{(g)} \leftrightarrow 2AlkAlO_2 \cdot xSiO_{2(s)} + 2HCl_{(g)} \quad (8)$$

107 Moreover, several studies have been conducted to model the capture of K-species on Al-Si additives in
108 literature [30]. However, the current models have some limitations. One common issue is that many
109 models do not have a maximum limit to the capture value, which makes them unsuitable for use in a
110 pulverised fuel power plant. Additionally, some models do not consider gas phase reactions (e.g. between
111 KCl and H_2O to form KOH), which can introduce errors when considering reactive species like KCl. Another
112 drawback is the lack of consideration for multicomponent sorption, where both KOH and KCl may be
113 present in the gas phase and could potentially compete with each other in sorption reactions.
114 Although it is a modest air pollutant, HCl gas is troublesome because of its high solubility and corrosive
115 nature [31, 32]. That is the reason why its removal is an important issue. Studies on Ca-based sorbents
116 indicated a high conversion rate for HCl between 400-650 °C [33–35]. Reactions 9 and 10 show the
117 mechanisms for HCl sorption on CaO.

$$CaO_{(s)} + 2HCl_{(g)} \leftrightarrow CaCl_{2\,(s)} + H_2O_{(g)} \quad (9)$$

$$CaCO_{3\,(s)} + 2HCl_{(g)} \leftrightarrow CaCl_{2\,(s)} + H_2O_{(g)} + CO_{2\,(g)} \quad (10)$$

Thermodynamic investigations have shown that only a concentration of 600 ppm_v can be achieved during HCl sorption on Ca-based sorbents above 800 °C [36]. However, in a dry atmosphere, HCl has been reduced below 1 ppm_v [37, 38] by stabilizing calcium in an aluminosilicate phase (hydrogrossular). Further studies are required to determine the HCl concentration achieved by the hydrogrossular in a humid reducing atmosphere [4]. Sufficient HCl removal with Na_2CO_3, K_2CO_3, and dried distillers grains with solubles (DDGS) ash has also been demonstrated for temperatures up to 550 °C at Forschungszentrum Jülich [39]. To determine kinetically effects, a gas stream consisting of 66 % He, 4 % H_2, and 30 % H_2O was varied between 2-4 l/min. The length of the sorbent fill varied from 25 mm to 100 mm. The HCl sorption on Na_2CO_3 and K_2CO_3 at temperatures between 400 °C and 550 °C showed that this reaction is kinetically limited. In order to prevent the limitation through kinetics, the space velocity has to be reduced to 4900 h^{-1} for the Na_2CO_3 sorbent and to 3750 h^{-1} for the K_2CO_3 sorbent. However, HCl concentrations of 1 ppm_v are achievable below these space velocities.

The aim of this work was to investigate suitable sorbents for hot gas cleaning downstream of the gasifier. The hot gas cleaning system should operate at 650 °C, just like the gasifier itself, in order to avoid heat losses. The fact that the stream leaving the gasifier has a low CO_2 concentration due to the reaction with CaO and a high H_2 concentration due to the water gas shift reaction was given special consideration when selecting suitable sorbents. Because the sorptive removal of KCl has already been tested with aluminosilicates at higher temperatures, this work focused more on the removal of H_2S.

2 Modeling and Experimental Section

A model for describing both the release and the removal of trace substances in syngases was created. The aim was to determine the limits of sorptive alkali and sour gas removal. For the thermodynamic

equilibrium calculations, FactSage [40] with the in-house developed oxide database GTKT [41] and the commercial database SGPS were used. While the model for the release calculations for several biomass fuels can be found in [42], Figure 1 shows the calculation scheme for the subsequent hot gas cleaning. The resulting gas compositions from the release model was used as input for the present calculations. The concept consists of an alkali and a sour gas cleaning unit. The gas is brought into contact with various sorption materials. The sorbents were added in stoichiometric excess, so that the resulting concentrations are the minimum achievable with the respective sorbents and temperature. Moreover, no further gas-solid reactions can occur. Since HCl is released during alkali cleaning with aluminosilicates (reaction 8), the sour gas cleaning unit must be located afterwards.

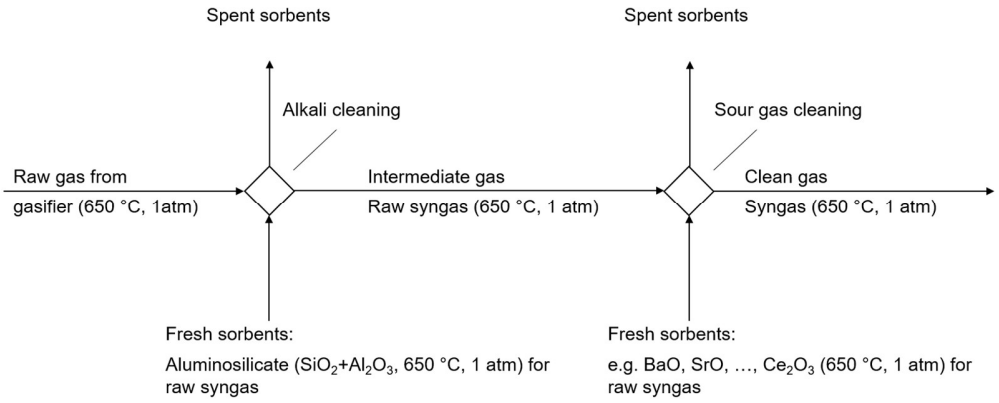

Figure 1: Schematic representation of the HGC calculations

2.1 Experimental setup and sorbent materials for KCl sorption

Except for the gas analysis, the experimental setups for the KCl sorption and the sour gas sorption were almost identical: A synthetically mixed syngas loaded with impurities was led through a sorbent bed in a tube furnace. This type of experimental setup has been used successfully in several previous studies [43–45]. All sorption experiments were conducted as fixed bed investigations at atmospheric pressure. The KCl sorption tests were stopped after 20 h since no increase in the corresponding signal could be detected.

158 The KCl sorption experimental setup consisted of a tube furnace with five independent heating zones. A
159 high-density Al_2O_3-tube was used as the reaction tube. This material does not bind any alkalis at
160 temperatures below 1000 °C. The KCl concentration was determined by molecular beam mass
161 spectrometry (MBMS) as described in detail in [18].
162 Since previous thermodynamic calculations showed that the substitution of a simulated flue gas by helium
163 has no influence on the KCl sorption [4, 46], the syngas was synthetically mixed from 10 % H_2 and 83 % He.
164 The gas stream was further loaded with 7 % H_2O by flowing through a vaporizer. The gas mix (4 l/min)
165 flowed through a flange into the cold end of the Al_2O_3 tube.
166 The Al_2O_3 tube had an inner diameter of 25 mm and a length of 870 mm. It was installed horizontally in a
167 5-zone furnace with an additional heating at the outlet. The additional heating was used to prevent the
168 KCl from condensing at the inlet of the MBMS. The syngas was loaded with approximately 25 ppm_v KCl
169 shortly after flowing into the Al_2O_3 pipe by overflowing a 750 °C hot Al_2O_3 boat filled with KCl (alkaline
170 source). The contact surface of the KCl with the syngas stream was approximately 900 mm^2.
171 The KCl loaded syngas then flowed through the bed of an aluminosilicate sorbent at 650 °C. To completely
172 cover the pipe cross-section with sorbent material, the sorbent was pressed between two Al_2O_3-frits. The
173 frits had a material thickness of 10 mm and consisted of a coarse-pored high-temperature Al_2O_3-foam. To
174 reduce the flow resistance the sorbent was fractionated to a grain size between 1.6 and 4 mm.
175 Approximately 30 g of sorbent were used per bed corresponding to a bed length of 50 mm.
176 The experimental setup such as syngas composition, syngas volume flow, general settings of the MBMS
177 (ionization voltage, multiplier voltage, optics) was kept constant.
178 The chemical composition and the specific surface areas of the sorbents are given in Table 2 and Table 3.
179 Before the BET measurement, the samples were outgassed by heating in a vacuum at 300 °C for 1 h. The
180 materials used for alkali sorption were aluminosilicates differing in Al_2O_3 and SiO_2 content. Except for the
181 bauxite, the SiO_2/Al_2O_3 ratio is bigger than 1. All sorbents listed in Table 2, except Boke Bauxite and Cat
182 litter, were prepared from powder. The powder was mixed with water and formed into pellets. The pellets

were then exposed in Al_2O_3 crucibles for 5 h at 650 °C in an air atmosphere. The sorbents were fractionated afterwards to a particle size of 1.6 to 4 mm. Cat litter and Boke Bauxite samples were still available from previous experiments and were only fractionated accordingly.

Table 2: Chemical composition of the KCl sorbents [wt-%]

Sorbent	Al_2O_3	SiO_2	Fe_2O_3	K_2O	Na_2O	CaO	MgO	BaO	Total
Boke-Bauxite	75	1.3	17.4	-	-	-	-	-	93.8
Clinoptilolite	12.8	76.2	0.3	3.5	1	2.3	0.6	0.1	96.8
Kaolin	47.2	58.6	0.8	2.2	0.1	0.1	0.3	-	109.4
Bentonite	17.9	64	1.1	0.5	3.1	0.4	2.8	0.1	89.9
Cat litter	0.2	51.1	-	-	-	20.3	2.2	-	73.9
Montmorillonite	19.5	61	0.9	1.4	0.3	0.6	3.7	-	87.4
Foam	94.1	5.5	-	0.5	0.5	-	0.1	-	100.7

Table 3: Specific surface areas [m^2/g] of the KCl sorbents

Sorbent	Specific Surface
Boke-Bauxite	240.387
Clinoptilolite	26.366
Kaolin	15.761
Bentonite	15.538
Cat litter	95.083
Montmorillonite	60.417
Foam	1.358

Calibration measurements were carried out to correlate the signal intensity measured at the MBMS with the respective KCl concentrations. The experimental setup corresponded to the one for KCl sorption, with the exception of the absence of sorbent. Furthermore, the temperature of the KCl source was increased

191 step by step over several empty tube measurements. The KCl concentration in the syngas of an empty
192 tube measurement was determined via the weight loss of the KCl source.
193 The masses 74 and 76 can be directly assigned to $K^{35}Cl^+$ and $K^{37}Cl^+$, respectively. Furthermore, the masses
194 35, 37, and 39 show the presence of the KCl fragments $^{35}Cl^+$, $^{37}Cl^+$, and $^{39}K^+$. Since chlorine reacts to HCl in
195 the presence of water, signals could also be measured on masses 36 and 38. On the masses 56 and 58,
196 which correspond to KOH and $K^{18}OH$ respectively, no significant signal increases could be observed. The
197 quantification of the potassium chloride was carried out via mass 39, since it has the highest intensity.
198

199 **2.2 Experimental setup and sorbent materials for H_2S and HCl sorption**

200 A test rig consisting of a glass reactor, various gas pipes and a water vaporizer was set up. A programmable
201 furnace (AGNI Wärme- und Werkstofftechnik GmbH, Model: GHT-130-40-400-5H) was used to obtain a
202 temperature-controlled operation for the sorption experiments. The furnace temperature was controlled
203 via a PID controller acting on the temperature from the thermocouple integrated in the furnace (closed-
204 loop control). Gas analysis was performed using mass spectrometry (MAX300, Extrel). The gas composition
205 in the H_2S-sorption experiments was set to 73% H_2, 13% Ar, 7% H_2O, 1% CO_2, 6% CO, 60 ppm_v. This
206 composition was based on FactSage-equilibrium calculations of a synthesis gas leaving a biomass gasifier
207 operated at 650 °C. Since the H_2S sorption can be influenced by several syngas components, the H_2S was
208 mixed in with CO (0.1 %). The inert components (N_2) and the hydrocarbons (mainly CH_4) were substituted
209 by Ar. Because of the expected low H_2S concentration of the gas after H_2S purification, the H_2S signal was
210 determined with an electron multiplier. For the remaining signals, a faraday detector was used.
211 The H_2S sorption measurements always proceeded in the same way. First, the glass reactor filled with
212 sorption material was flooded with argon. In the second step, the reactor was disconnected from the gas
213 supply by closing the valves immediately upstream and downstream of the reactor. The argon gas flow
214 was then used to purge the pipelines (the gas flow was not yet loaded with water). The CO/H_2S supply was
215 then started. Since the H_2S molecule adsorbed well on surfaces, a steady-state signal was obtained by

waiting until the H_2S signal plateaued. Next, the CO_2 stream and the H_2 stream were switched on. The valve to the water supply was opened and the heating of the water started. The gas flow is thus directed onto the water surface from above. After the first steam bubbles appeared, the gas (H_2, CO_2, Ar) was directed through the water and loaded. Subsequently, the gas mixture was passed through the reactor. As soon as the sorption material was saturated and the H_2S and HCl concentration increased, the sorption experiments were stopped. At the end of each experiment, the water supply was stopped and the reactor was flooded with argon.

Similar to the KCl sorption experiments, the HCl contamination was generated by evaporating a solid, i.e., NH_4Cl, in an Al_2O_3 boat at a fixed temperature during the experiment. The filled boat was attached to the glass rod of the reactor with a metal wire. To fix the sorption material in the glass tube, a foam was used as in the KCl sorption experiments (see Figure 2).

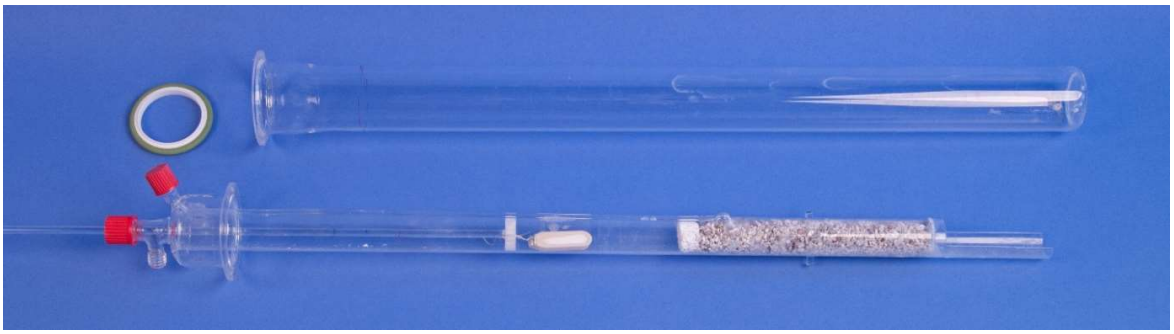

Figure 2: Glass reactor filled with SrO with additional HCl source

The experimental setup for HCl sorption differed only slightly from the experimental setup for H_2S sorption: Helium was used here for the substitution of CH_4 and N_2. This change was made because Ar has isotopes at masses 36 and 38 in addition to the main mass at 40. The main signal of HCl is at mass 36.

Since the temperature profile inside the furnace was very steep, the NH_4Cl was evaporated upstream the furnace via a heating belt.

Table 4 lists all the chemicals used for HCl and H_2S sorption. The degree of purity was over 98 % for all chemicals. The sorption properties of a commercially available lime (Sorbacal) from Rheinkalk were also

investigated. The chemical composition is given in Table 5. The values for the oxides were calculated from the elements measured with ICP-OES. In previous studies, the CaO content was 98.1 wt-%. The lower percentage can be explained by the fact that $Ca(OH)_2$ and $CaCO_3$ have formed during storage.

Table 4: List of chemicals used for H_2S and HCl sorbents preparation

Chemical	Assay	Supplier	CAS Registry Number
$BaCO_3$	≥ 99%	Thermo Scientific, Schwerte	513-77-9
$CaCO_3$	≥ 99.5 %	Thermo Scientific, Schwerte	471-34-1
CeO_2	≥ 99.5%	Thermo Scientific, Schwerte	1306-38-3
La_2O_3	≥ 99.9 %	Thermo Scientific, Schwerte	1312-81-8
$SrCO_3$	≥ 98 %	Fischer Scientific, Geel (Belgium)	1633-05-2
Y_2O_3	≥ 99 %	Merck, Darmstadt	1314-36-9
Zn_2TiO_4	≥ 99.9 %	Thermo Scientific, Schwerte	12036-43-0

Table 5: Chemical composition of Sorbacal [wt-%]

Sorbent	Al_2O_3	SiO_2	Fe_2O_3	CaO	MgO
Sorbacal	0.2	1	0.2	62.1	0.6

In order to ensure a concentration of 1 ppm_v H_2S in the syngas, conventional sorption materials like ZnO could not be used, as these only show good sorption efficiency at temperatures below 600 °C. Therefore, the Sr- and Ba-based sorption materials developed by Stemmler at Forschungszentrum Jülich were included in the experiments. Stemmler's calculation showed that stabilized Ba-based sorbents keep the 1 ppm_v concentration even in a temperature range between 800 °C and 900 °C [39].

There is a slight solubility of BaO and CaO at temperatures above 1200 °C [4, 47, 39]. Moreover, all CaO-SrO mixtures above 900 °C are forming a CaO-SrO solution phase. Since increased marginal solubilities exist, mixtures of 90 mol-% CaO and 10 mol-% SrO (or BaO), respectively 10 mol-% CaO and 90 mol-% SrO were used for H_2S sorption.

For the preparation of the H_2S and HCl sorbents, raw powder ($SrCO_3$, $ZnTi_2O_4$, CeO_2, …) was mixed with water and formed to pellets. For the preparation of the Sr- and Ba-based sorption material, carbonates were used. Preliminary thermo-gravimetric measurements showed that the decomposition reaction of $CaCO_3$ to CaO is completed at about 800 °C to 850 °C, while $SrCO_3$ is completely decomposed at about 1150 °C and $BaCO_3$ at 1200 °C. Therefore, the sorbents used in the sorption experiment were prepared at 1600 °C in platinum crucibles.

For the production of reduced ceria sorption material, raw powder of CeO_2 was mixed with water and heated in a 10% H_2-Ar atmosphere at 1500 °C for 72 h. Ce_2O_3 is stable in air if it has been produced at temperatures above 1400 °C [48]. The specific surface area of the most highly reduced cerium oxide sample was determined to be 0.21 m^2/g.

The temperatures and exposure times of the other sorbents can be found in Table 6. To ensure a certain mechanical stability of the sorption material, different temperatures and dwell times in the furnace were used depending on the sorption material. The specific surface areas of the sorbents are listed in Table 8.

Table 6: Manufacturing temperatures and duration

Sorbent	Temperature [°C]	Duration [h]
La_2O_3	1400	5
Zn_2TiO_4	650	5
CeO_2	1050	10
Y_2O_3	1050	10

Table 7: Specific surface areas of the H_2S and HCl sorbents [m^2/g]

Sorbent	Specific surface
Sorbacal	4.778
La_2O_3	0.642
Zn_2TiO_4	0.586
Y_2O_3	1.761
90Ca10Ba	0.878
90Ca10Sr	0.242
10Ca90Sr	0.466
100Sr	0.209

As described earlier, the H_2S signal was recorded by mass spectrometry. Before starting the H_2S investigations, the signal intensities were correlated with the corresponding H_2S concentrations. In analogy to the KCl calibration, empty pipe measurements were carried out.

Since a syngas purity of less than 1 ppm_v H_2S was aimed for, H_2S concentrations of 60 ppm_v, 30 ppm_v, 10 ppm_v, 5 ppm_v, 2.5 ppm_v, 1 ppm_v, and 0 ppm_v were chosen as calibration points. Since H_2S was mixed with CO, a decrease in the H_2S input was accompanied by a decrease in the CO input. The syngas fraction missing due to the reduction of the H_2S concentration was substituted by Ar. A total flow rate of 2 l/min was used for the calibration. The empty tube measurements resulted in a linear correlation between H_2S concentration and signal intensity at mass 34.

According to the KCl and H_2S calibration, a correlation between signal intensities and HCl concentrations was conducted prior to the HCl sorption experiments. An empty pipe calibration was carried out similar to the KCl calibration.

3 Results and Discussion

3.1 Modeling results

Depending on biomass, the syngas leaving the gasifier contains approximately 20 ppm_v H_2S, 160 ppm_v HCl, and up to 22 ppm_v alkali chlorides [42]. After sorptive alkali hot gas cleaning on aluminosilicates at 650 °C, the NaCl concentrations ranged up to 0.97 ppb_v, while the maximum KCl concentration was 1.5 ppb_v. With concentrations of up to 188 ppm_v, in the purified syngas, the concentration of HCl was the only chlorine species that increased significantly according to reaction 8. Since H_2S does not react with aluminosilicates, its concentrations remained unchanged at 20 ppm_v.

Based on the results of the alkali cleaning calculations, further calculations for the sour gas cleaning were carried out. Therefore, several metals/metal oxides as well as natural occurring alkali and alkaline earth compounds had been considered.

The results (Figure 3) show that SrO, BaO, and Ce_2O_3 were suitable to reduce the concentrations of H_2S from approximately 20 ppm_v to values below 1 ppm_v (SrO: 2.8 ppb, BaO, 0.013 ppb, Ce_2O_3: 1 ppt) at 650 °C. These concentrations were all within the range of purities demanded for the use of SOFC in Table 1. From a thermodynamic point of view, gas purification can therefore be carried out in the way described. With the help of Zn-based sorption materials (ZnO and Zn_2TiO_4), the H_2S concentration could be reduced to a few ppm_v (ZnO: 5.1 ppm_v, Zn_2TiO_4: 10.4 ppm_v) at 650 °C.

Similar statements can also be made about the HCl sorption at 650 °C with the sorption materials mentioned. BaO and SrO sorbents could reduce the concentrations of HCl from around 188 ppm_v to 2.8 ppb_v and 0.37 ppm_v. Ce_2O_3 reduced the HCl amount to 17.7 ppm_v, while ZnO and Zn_2TiO_4 were not able to reduce the input concentration as expected. Figure 3 shows another positive effect of BaO, SrO, and Ce_2O_3 on the syngas. The CO_2 concentrations of approximately 1% could be further reduced. This also has the advantage of shifting the equilibrium to higher H_2 concentrations.

The sorption capacity of BaO- and SrO-based sorption materials with respect to CO_2, H_2S, and HCl can be seen positively over a wide temperature range (400-1000 °C). Ce_2O_3, on the other hand, lowered the HCl concentration significantly only up to about 700 °C.

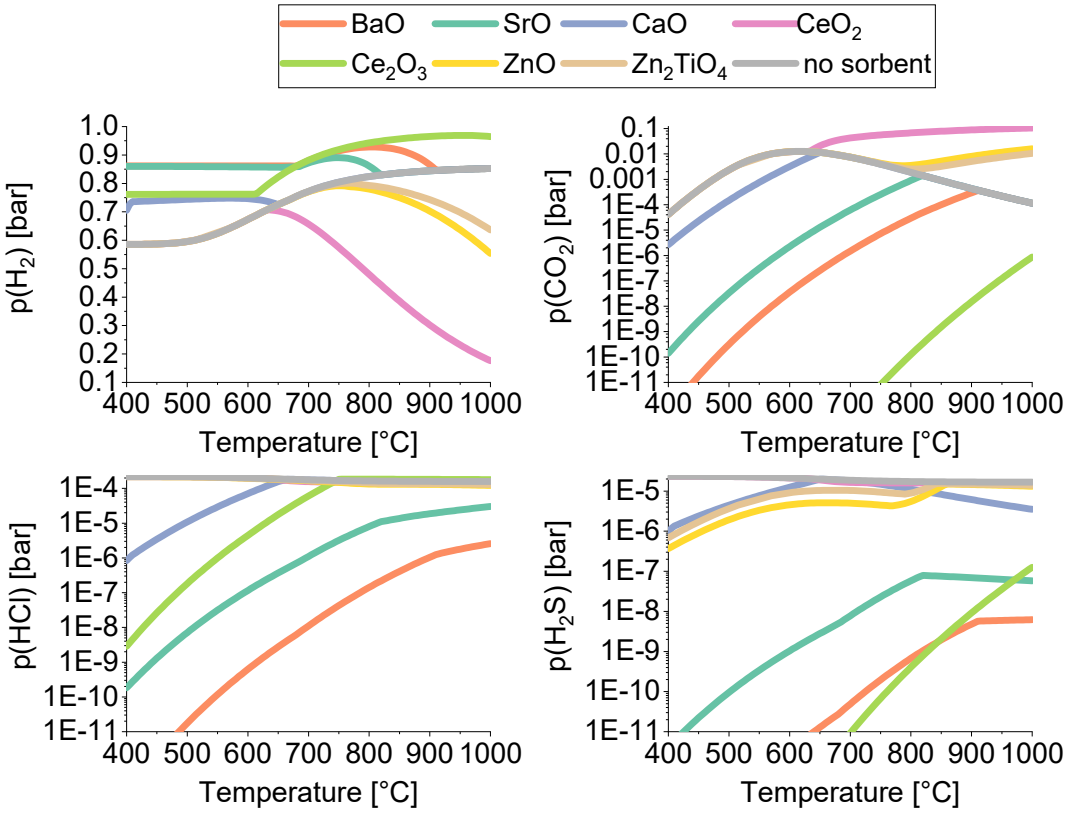

Figure 3: Partial pressure of H_2, CO_2, HCl, and H_2S after H_2S/HCl cleaning for different sorbents

According to these calculations, the barium, strontium, and cerium-based sorption materials result in low H_2S and HCl concentrations. They are also temperature-stable at 650 °C and will be therefore investigated experimentally in the following.

3.2 Experimental KCl sorption at 650 °C

As described, in all investigations for the KCl removal, a KCl-loaded syngas, was passed through a fixed bed. The achievable KCl concentration was determined in situ using a MBMS. Reaction 8 shows a

dependence on the water content of the KCl concentration in the syngas. The gas mixture used in these experiments (83% He, 10% H_2, and 7% H_2O) is thus a permissible simplification of the GICO syngas.

Figure 4 shows the KCl concentration profiles of different sorbents. All tested sorbents reduced the KCl concentration to as low as 0.4 ppm_v and thus, are suitable sorbents. The KCl concentrations when using Kaolin, Bentonite, Montmorillonite, and Clinoptilolite were below the detection limit.

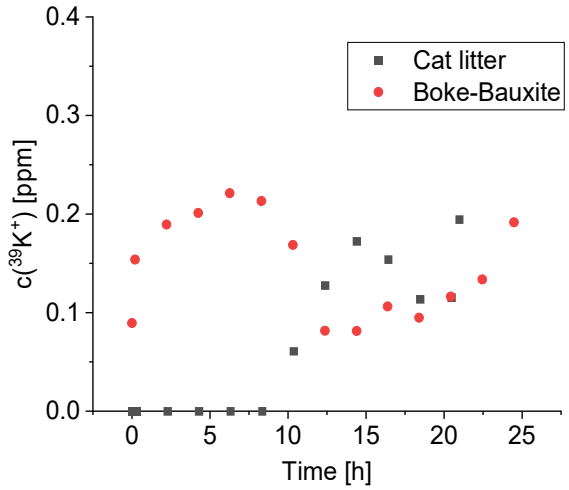

Figure 4: KCl concentration after streaming through a sorbent bed at 650 °C (inlet concentration: 83% He, 10% H_2, 7% H_2O, and 25 ppm_v KCl, $\dot{V}_{tot}$ = 4 l/min, 30 g sorbent)

3.3 Experimental H_2S sorption at 650 °C

In all investigations on H_2S cleaning, the syngases were passed through a fixed bed. The H_2S signal of the purified gas was recorded by mass spectrometry (MS). Stemmler reported considerable delays in his measurements since the H_2S molecule adsorbed well on surfaces [4]. Therefore, in this work the gas was fed into a separate circuit so that the surfaces of the gas pipes were saturated with H_2S until shortly before the glass reactor. To shorten the saturation time, the H_2S concentration in the gas was increased before opening the sorbent circuit. The experiment was started as soon as there was a steady-state signal.

In order to obtain a rough overview of the sorption behavior of the different sorbents, sorption experiments were carried out at a high flow rate (2 l/min). The most promising sorbents were then tested

at a lower flow rate (200 ml/min) and with a longer sorption fill (100 g sorbent). Figure 5 shows the H_2S concentrations during the first 20 minutes of the H_2S sorption experiments for different sorbents. The CO_2 intensity was also recorded. However, since the CO_2 concentration was not in the main focus of the investigations, the MS was not calibrated for CO_2 and the values are given as signal intensities, only.

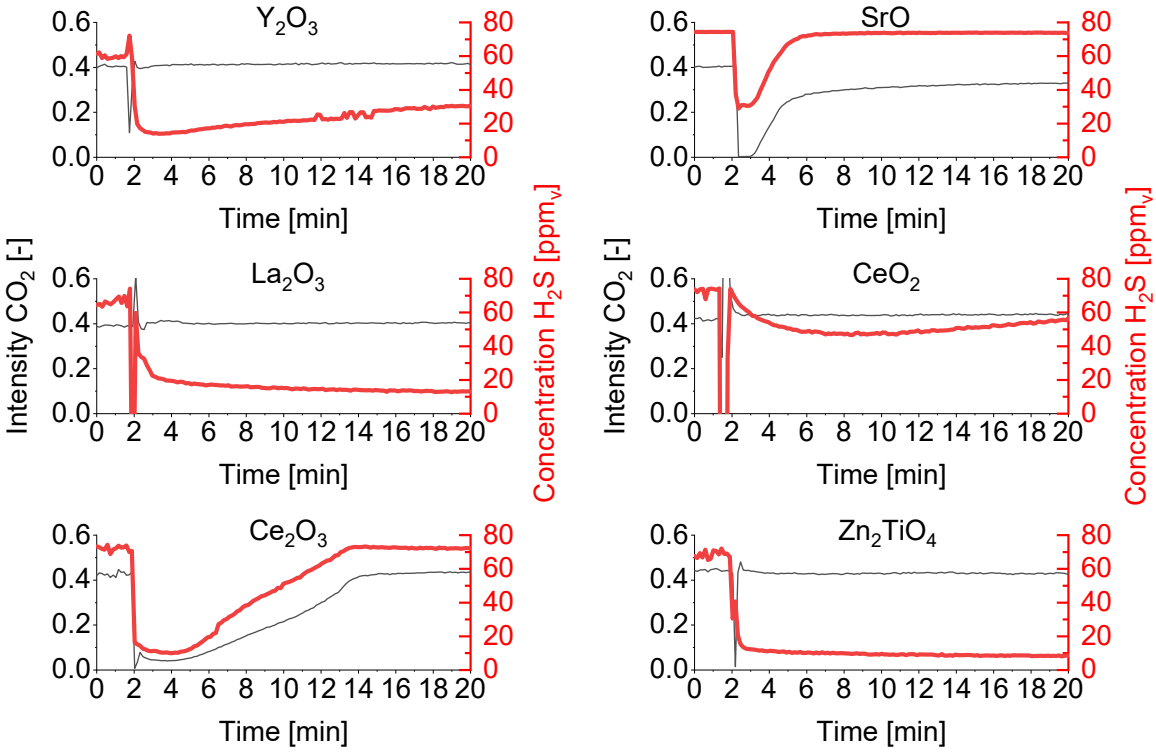

Figure 5: Results of the mass spectrometric investigations: CO_2 intensity and H_2S concentrations [ppm_v] of different sorbents. Inlet concentration: 73% H_2, 13% Ar, 7% H_2O, 1% CO_2, 6% CO (60 ppm_v H_2S), T = 650 °C, $\dot{V}_{tot}$ = 2 l/min, 30 g sorbent

Although CO_2 leaves the gasifier with a low concentration of around 1 % due to the sorption with CaO (calculated thermodynamic equilibrium), SrO and Ce_2O_3 decreased the concentration even a little further. However, a rise in the CO_2 signal could be observed after just a few minutes for these sorption materials. Parallelly, the H_2S concentration increased. Therefore, CO_2 can be seen as a limiting factor in the conducted H_2S-sorption experiments: SrO reacts with CO_2 to form a carbonate ($SrCO_3$) while the reduced cerium oxide

346 (Ce_2O_3) oxidizes (CeO_2). Both, the oxidation of the Ce_2O_3 and the carbonatization of SrO took place quickly,
347 which is the reason that H_2S could only be removed well for a short time.
348 For Zn_2TiO_4 no decrease of the CO_2 signal could be seen, as $ZnCO_3$ is only stable at temperatures up to
349 approximately 300 °C. Zn_2TiO_4 lowered the H_2S concentration to single-digit ppm_v values for several hours
350 despite a high flow rate. Because La_2O_3 has similar properties compared to Ce_2O_3 (molar mass,
351 electronegativity), which according to the literature has a good H_2S sorption effect [21, 49, 50], it was also
352 used in the experiments. Since the 3-valent form of Lanthanum oxide (La_2O_3) and Yttria (Y_2O_3) are stable
353 under gasification conditions, the CO_2 signals remained constant. However, H_2S concentrations for La_2O_3
354 were as low as for Zn_2TiO_4. Moreover, La_2O_2S was detected after the sorption experiment using XRD.
355 As the H_2S signal for SrO and Ce_2O_3 did not reach a plateau during sorption, it can be assumed that the gas
356 has not yet reached its achievable purity. In order to give a better estimate of the sorption capacity,
357 experiments were carried out with a reduced volume flow rate and a longer sorbent bed (100 g).
358 Furthermore, a stabilizing effect of CaO on SrO against carbonization was investigated by testing mixtures
359 of 10 mole-% CaO, 90 mole-% SrO (10Ca90Sr), and 90 mole-% CaO, 10 mole-% SrO (90Ca10Sr). In addition,
360 a 10 mole-% BaO, 90 mole-% CaO (90Ca10Ba) mixture was tested because it has achieved good results in
361 Stemmler's work [10].
362 Figure 6 (left) shows the H_2S concentration when cerium oxide (Ce_2O_3) is used. H_2S concentrations of less
363 than 1 ppm_v could be achieved for more than 5 hours. After saturation, an extreme increase in the H_2S
364 concentration (approximately 170 ppm_v) could be seen for a short time, which slowly decreased. This is
365 due to the fact that H_2S was released again. The oxidized form (CeO_2) was more stable than the sulfides
366 formed (Ce_2O_2S, Ce_2S_3).
367 The XRD analysis of the sorption material after the sorption experiment showed a single CeO_2 phase. No
368 more sulfides or reduced cerium oxides could be detected.

The sorption with the BaO-sorbent (10Ba90Ca) also showed an increase in the H_2S concentration above the initial concentration of 60 ppm_v after deactivation of the sorption material (Figure 6, right). The sorbent was also able to keep the H_2S concentration below 1 ppm_v for approximately 3 h.

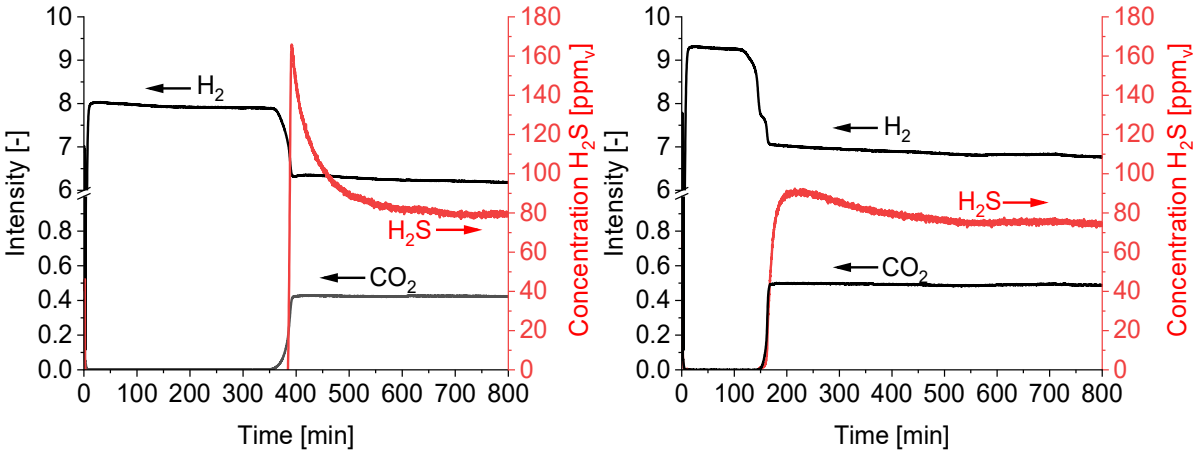

Figure 6: Results of the mass spectrometric investigations: CO_2 intensity and H_2S concentrations [ppm_v] of Ce_2O_3 (l.) and 10Ba90Ca (r.). Inlet concentration: 73% H_2, 13% Ar, 7% H_2O, 1% CO_2, 6% CO (60 ppm_v H_2S), T = 650 °C, $\dot{V}_{tot}$ = 0,2 l/ min, 100 g sorbent

Since both the Ba-sorbent and the Ce-sorbent also reacted with CO_2, the thermodynamic equilibrium shifted in the direction of extremely high hydrogen concentrations. However, no sulfide could be detected after the experiment due to the release of H_2S after sorption. The XRD analysis of the sorption material showed that the formation of $CaCO_3$ was suppressed and that only $BaCO_3$ and CaO (Lime) were present (see Figure 7).

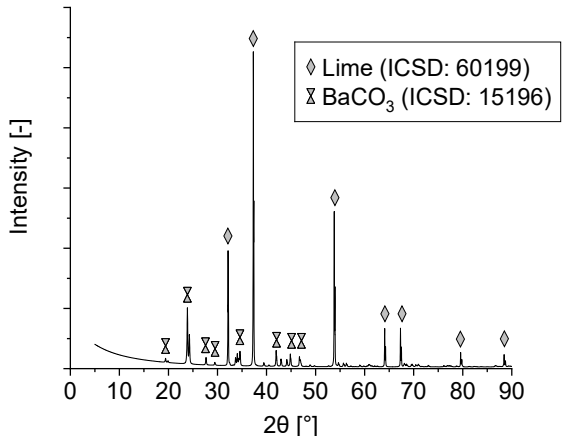

381

382 **Figure 7: XRD spectrum of 10Ba90Ca after sorption experiment**

383 As already described, 1 % CO_2 was selected for the input concentration in the experiments, because this is
384 the minimum CO_2 concentration that can be achieved with CaO at 650 °C. Thus, it is confirmed that BaO
385 in the sorbent was reducing the CO_2 concentration further.

386 To gain a better understanding of the deactivation behavior of 10Ba90Ca over time, the sorption
387 experiment was stopped after 50, 100, 150, and 600 minutes. At these times, the syngas was replaced by
388 argon. After the furnace had cooled down, the fixed bed was divided into ten fractions of equal size for
389 chemical analysis.

390 Figure 8 shows the evaluation of the elemental analysis. Sample position 1 refers to samples taken at the
391 gas inlet side, while sample position 10 are samples taken at the gas outlet side.

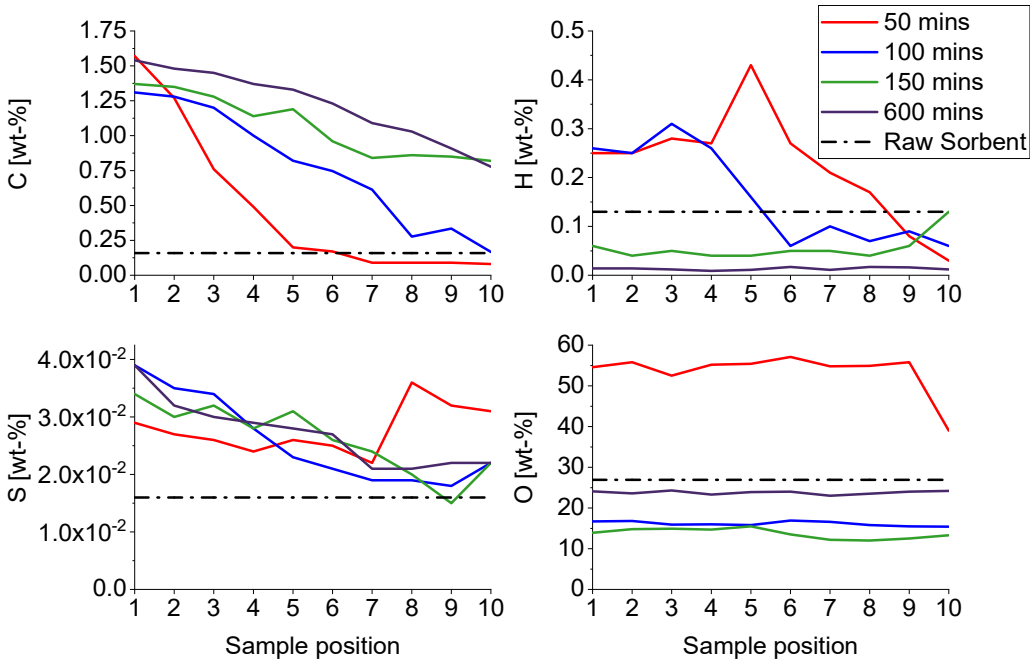

392

393 **Figure 8: Elemental analysis of 10Ba90Ca after 50, 100, 150, and 600 minutes of sorption time**

394 It can clearly be seen that the C concentrations increased with increasing residence time in the reactor.
395 Furthermore, higher C concentrations were observed at the reactor inlet. The C-analysis of an unloaded
396 reference sample (dotted line) show that hardly any carbonates were present after sorbent production.
397 Since only gases such as CO_2 and CO were present as carbon sources, the increase in C concentration was
398 due to the formation of $BaCO_3$ ($CaCO_3$ was not formed under these conditions). The higher C
399 concentrations at the reactor inlet (sample position 1) compared to the reactor outlet (sample position
400 10) were due to the higher CO_2 concentrations at the reactor inlet. Lower amounts of CO_2 arrived at the
401 back of the reactor with a time delay. After 50 minutes, approximately 50 % of the sorption material has
402 reacted to $BaCO_3$.
403 For the sulfur concentration, there was also a corresponding drop in concentration along the bed. Only
404 after 50 minutes an increase of the sulfur concentration for the samples that were located close to the gas
405 outlet (sample positions 8-10) could be observed. Since the sulfur concentration at positions 8-10 has
406 decreased over time while the C concentration has increased, it is reasonable to assume that the

carbonates were more stable than the sulfur compounds and that the sulfur components (BaS) were driven further to the gas outlet. However, the leaching of the sulfur components did not occur completely. Figure 9 shows the H_2S sorption process when using SrO. The 1 ppm_v H_2S target could not be achieved here. In contrast to Ce_2O_3 and the Ba-based sorption material, there was no extreme increase in the H_2S concentration after deactivation by the CO_2.

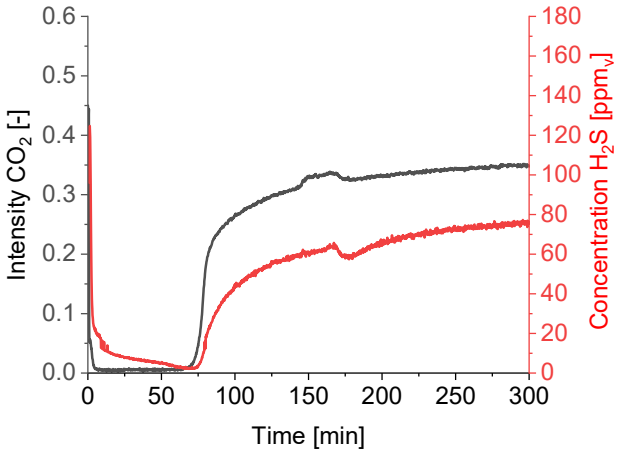

Figure 9: Results of the mass spectrometric investigations: CO_2 intensity and H_2S concentrations [ppm_v] of SrO. Inlet concentration: 73% H_2, 13% Ar, 7% H_2O, 1% CO_2, 6% CO (60 ppm_v H_2S), T = 650 °C, $\dot{V}_{tot}$ = 0,2 l/min, 100 g sorbent

Figure 10 shows that $SrCO_3$ has been formed. Nevertheless, SrO could still be detected in the sample by XRD. Possibly only an external $SrCO_3$ layer has been formed. The inner part of the sorbent could still consist of SrO after the sorption experiment since the SrO sorbent had a small specific surface area (0.209 m^2/g, see Table 8).

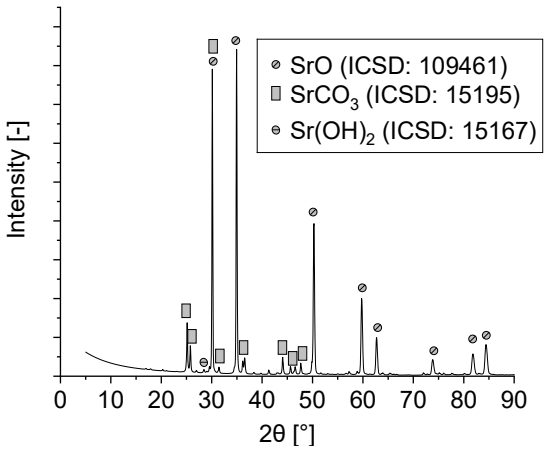

420

421 **Figure 10: XRD spectrum of SrO after sorption experiment**

422 Figure 11 shows the effect of CaO in a CaO-SrO mixture on the H_2S concentration. It can be seen that in a
423 CaO rich sorbent material (90Ca10Sr) the CO_2 concentration increased after a few minutes. As explained
424 earlier, CaO cannot reduce CO_2 any longer. Since CO_2 and H_2S intensities did not run parallel for both
425 90Ca10Sr and 10Ca90Sr, it is assumed that a mixed phase was present that reduced sulfur well. The XRD
426 analysis of 90Ca10Sr showed that three $Ca_{1-x}Sr_xO_2$ mixed crystal phases were present, two rich in Ca with
427 a=4.838 Å and 4.859 Å and one rich in Sr with a=5.112 Å.

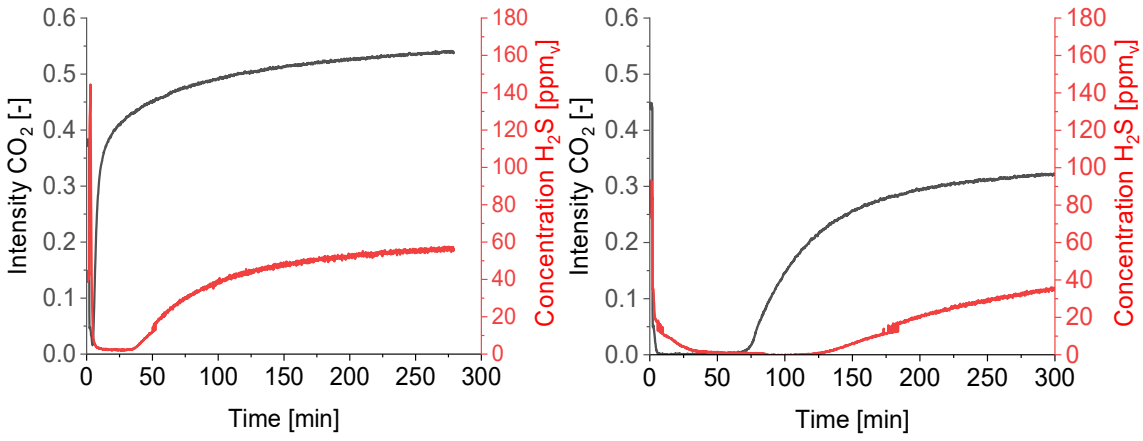

428

429 **Figure 11: Results of the mass spectrometric investigations: Influence of CaO on the stabilization of the**
430 **Sr-sorbent. CO_2 intensity and H_2S concentrations [ppm_v] of 90Ca10Sr (l.) and 10Ca90Sr (r.). Inlet**
431 **concentration: 73% H_2, 13% Ar, 7% H_2O, 1% CO_2, 6% CO (60 ppm_v H_2S), T = 650 °C, $\dot{V}_{tot}$ = 0,2 l/min,**
432 **100 g sorbent**

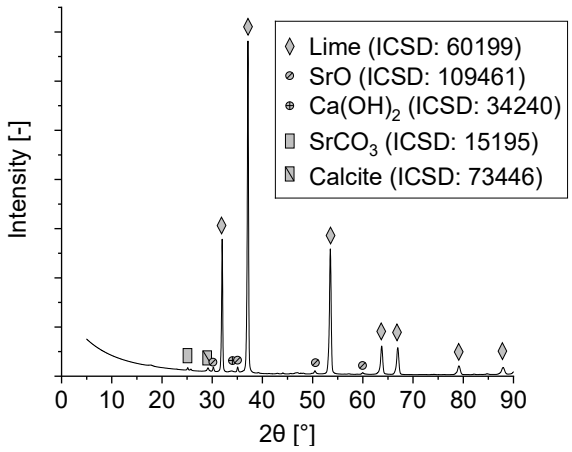

433

434 **Figure 12: XRD spectrum of 90Ca10Sr after sorption experiment**

435 **3.4 Experimental HCl sorption at 650 °C**

436 For the HCl sorption experiments, the two sorbents with the lowest equilibrium concentration according
437 to model calculations (10Ba90Ca and SrO) were used. Similar to the KCl sorption experiments, the
438 contamination was generated by evaporation of a source. In order to prevent the BaO sorption material
439 from being deactivated by CO_2 during the heating phase of the NH_4Cl, the heating tape was turned on 7 h
440 before the gas was passed through the glass reactor. Thus, HCl concentrated in the reactor and the
441 equilibrium plateau was reached after only a few minutes. Compared to the H_2S measurement (see Figure
442 6, right), the HCl sorption showed an earlier increase of CO_2 after only 20 minutes (see Figure 13, left).
443 As in the H_2S sorption experiments, the sorption material in the HCl sorption experiments was deactivated
444 by CO_2 in the syngas. The HCl signal in the 90Ca10Ba sorption measurement "shot up" beyond the input
445 concentration and decreased again. This is similar to the H_2S sorption measurement. It indicates that HCl
446 was released.
447 The experimental procedure for SrO deviated a little. Here the heating tape, which was used for the
448 evaporation of the NH_4Cl, was switched on two minutes before the glass reactor was opened. Since pure
449 SrO was used here, the deactivation time was longer than for the Ba-based sorbent (see Figure 13, right).
450

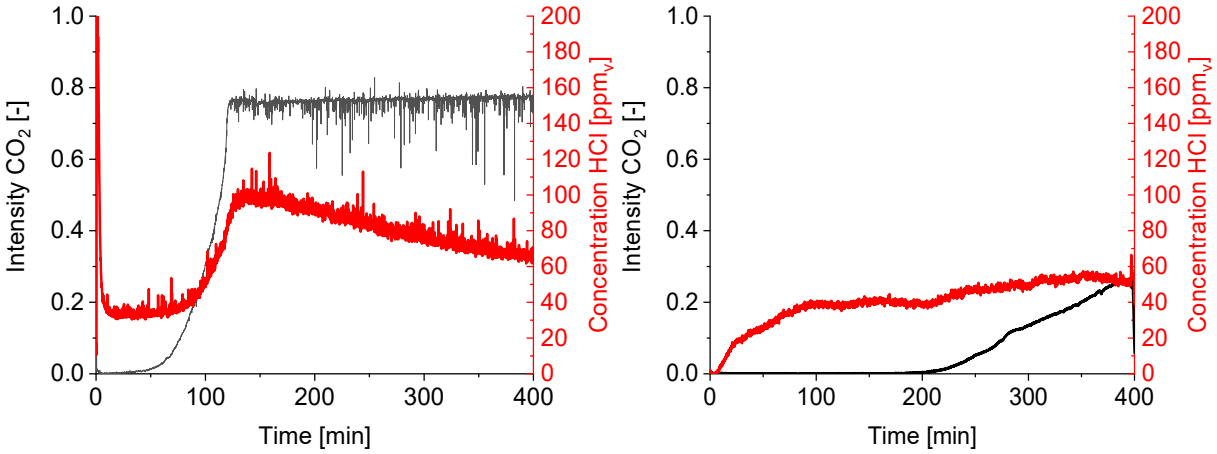

Figure 13: Results of the mass spectrometric investigations: CO_2 intensity and HCl concentrations [ppm_v] of 10Ba90Ca (l.) and SrO (r.). Inlet concentration: 73% H_2, 13% Ar, 7% H_2O, 1% CO_2, 6% CO, 50 ppm_v HCl, T = 650 °C, $\dot{V}_{tot}$ = 0,2 l/min, 100 g sorbent

The tested sorbents were not able to noticeably reduce HCl concentrations. Both sorption materials could only reduce the HCl concentration for a short time by about 10-20 ppm_v: 10Ba90Ca lowered the HCl concentration for about 50 minutes from about 50 ppm_v (input concentration) to about 30 ppm_v, SrO for about 100 minutes from about 50 ppm_v (input concentration) to 40 ppm_v.

Moreover, neither for 10Ba90Ca, nor for SrO, Cl phases could be detected via XRD after the experiment. This is due to the low HCl concentration in the syngas and the short deactivation time. Therefore, the samples were analyzed with EDXRF. Chlorine could be detected in all samples. However, only a semi-quantitative observation was possible. In contrast to the spectral lines of the other elements, the intensity of the chlorine K-alpha line varied strongly, indicating inhomogeneous chlorine distribution in the sample.

3.5 Comparison of the FactSage model with experimental observations

Aluminosilicates showed good reduction potential for the alkali compounds KCl and NaCl in the calculations. This could be confirmed by the laboratory experiments with MBMS. The tested aluminosilicates reduced the KCl concentration to levels well below 1 ppm_v in the experiments.

Similar observations could be made for the H_2S sorption. According to the calculations, Ce_2O_3, BaO, and SrO ccould significantly reduce the H_2S concentration below 1 ppm_v. This was also verified by the fixed bed sorption experiments. However, since the detection limit of the used mass spectrometer is about 1 ppm_v, no conclusions can be drawn about the exact actual purities of the gas for these three sorption materials. An increased H_2 concentration was also predicted for all three sorbents, which was also experimentally demonstrated. In comparison to the materials mentioned above, Zn_2TiO_4 was used as a conventional sorbent. Calculations and experiments proved that there is no deactivation by CO_2 here. The H_2S concentration achieved in the sorption experiment was also within the range of the model (1-10 ppm_v). Only the experiments for HCl sorption deviated strongly from the predictions. The tested sorbents could not really reduce HCl. This may be due to incorrect or insufficient data in the database and the non-consideration of kinematic effects, since only equilibria were covered by the model.

3.6 HGC concept for the GICO process

The present results indicate that the reduction of H_2S at 650 °C using either Ce_2O_3, SrO or BaO is only possible if the syngas has a low CO_2 content, since these sorbents are deactivated by carbonation or oxidation. Therefore, a low CO_2 content is beneficial when utilizing Ce_2O_3, SrO or BaO for high-temperature sorption. However, the GICO experimental plant may not achieve this theoretical value in its fluidized bed. CO_2 concentrations between 3-5 % are expected. To address this, a CO_2 polishing reactor that could decrease the CO_2 content can be added to the HGC unit of the gasifier side (see Figure 14).

Since aluminosilicates were able to reduce the alkali concentrations to the sub ppm_v range in the sorption experiments at 650 °C, the gas does not have to be cooled down before alkali cleaning. Since HCl is released during alkali binding into aluminosilicates (reaction 8), HCl cleaning must be carried out downstream in the process. A hot gas filter to remove particles is integrated after the alkali cleaning unit operating at 650 °C. It is important that the alkali cleaning is carried out before the filter so that it does not become clogged due to the condensation of alkali components. Afterwards, the gas reaches the H_2S sorption reactor

utilizing Ce_2O_3, BaO-, or SrO-based sorbents. To ensure the cracking of tar, which is not subject of the present investigations, the gas is lead through another reactor operating at 650 °C. Since a sufficient HCl reduction by BaO- or SrO-based sorbents could not be confirmed experimentally, adsorption by alkali carbonates is proposed. For successful HCl purification with Na_2CO_3, the temperature has to be lowered to 450 °C in a heat exchanger. At temperatures above 550 °C the sorption of HCl is not feasible as Na-based sorbents will release some of the chlorine as NaCl. The gas temperature can then be adjusted in another heat exchanger according to the conditions of the downstream equipment.

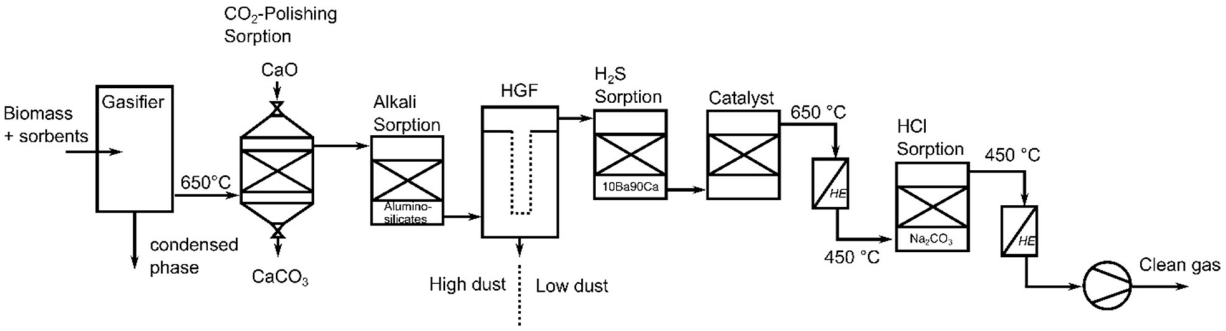

Figure 14: Layout of a HGC for the GICO process

4 Summary and Conclusions

Equilibrium calculations with FactSage were conducted for the hot gas cleaning unit of the GICO gasifier, proving that SrO- and BaO-based sorbents not only sufficiently reduced the H_2S, but also the HCl concentration into the sub ppm_v range. Furthermore, aluminosilicates could reduce the concentration of alkali chlorides below 1 ppm_v.

In order to verify the modeling results, a test rig has been set up for sour gas sorption (H_2S+HCl) using different metal oxides in a fixed bed. In this work, a simultaneous recording of the intensity and concentration curves of CO_2, H_2S and H_2 was achieved using mass spectrometry. Furthermore, water was used in all sorption experiments, which counteracts the binding of H_2S (reaction 1). With this setup, a reduction of the inorganic trace substance H_2S below 1 ppm_v could be detected for several hours (Ce_2O_3: 5 h, 90Ca10Ba: 2 h) at 650 °C which is considered sufficient to prevent catalyst poisoning. Ce_2O_3 and

90Ca10Ba can therefore be recommended for H_2S sorption from a thermodynamic point of view. Moreover, due to the simultaneous reaction between Ce_2O_3, respectively BaO, and CO_2, a further shift to higher hydrogen concentrations could be observed by the water gas shift reaction. Zinc titanate, the most effective conventional sulfur sorbent tested, only reduced H_2S levels to around 7 ppm_v.

On the other hand, 90Ca10Ba was not able to reduce the HCl concentration to a large extent. Concentrations could only be reduced from 50 to 40 ppm_v. Thus, contrary to initial thermodynamic calculations, this sorbent cannot be recommended for the sorption of H_2S and HCl simultaneously. The reasons for this phenomenon require further investigation. It may be related to the reaction kinetics between HCl and the sorption material, or it could indicate a need for improvements to the database. Consequently, it is proposed to remove HCl in a separate cleaning step at lower temperatures, e.g., on alkali carbonates at 450 °C.

It was found that six aluminosilicates were effective in reducing KCl levels to below 1 ppm_v, with four of them achieving concentrations below 400 ppb_v after 20 hours at 650 °C. Since HCl is released when KCl is embedded using aluminosilicates, it is advisable to remove KCl before HCl.

5 Acknowledgements

This work has received funding from the European Union's Horizon 2020 research and innovation program (Grant Agreement No.: 101006656). Further information are available at: https://www.gicoproject.eu/. We thank the colleagues of ZEA 3 of Forschungszentrum Jülich for chemical analysis.

5.1 References

1. Ngo T, Chiang KY, Liu CF et al. (2021) Hydrogen production enhancement using hot gas cleaning system combined with prepared Ni-based catalyst in biomass gasification. International Journal of Hydrogen Energy 46(20): 11269–11283. doi: 10.1016/j.ijhydene.2020.08.279

2. Marcantonio V, Müller M, Bocci E (2021) A Review of Hot Gas Cleaning Techniques for Hydrogen Chloride Removal from Biomass-Derived Syngas. Energies 14(20): 6519. doi: 10.3390/en14206519
3. Buchireddy PR, Peck D, Zappi M et al. (2021) Catalytic Hot Gas Cleanup of Biomass Gasification Producer Gas via Steam Reforming Using Nickel-Supported Clay Minerals. Energies 14(7): 1875. doi: 10.3390/en14071875
4. Stemmler M (2010) Chemische Heißgasreinigung bei Biomassevergasungsprozessen. Fakultät für Maschinenwesen. RWTH Aachen University, PhD-Thesis. Schriften des Forschungszentrums Jülich : Reihe Energie & Umwelt, Bd. 90, Aachen
5. Porbatzki D, Stemmler M, Müller M (2011) Release of inorganic trace elements during gasification of wood, straw, and miscanthus. Biomass and Bioenergy 35: S79-S86. doi: 10.1016/j.biombioe.2011.04.001
6. European Union (2021) Homepage GICO Project-GICO Process. Accessed 14.07.2024. https://www.gicoproject.eu/gico-process/. Accessed 14 Jul 2024
7. Westmoreland PR, Harrison DP (1976) Evaluation of candidate solids for high-temperature desulfurization of low-Btu gases. Environ. Sci. Technol. 10(7): 659–661. doi: 10.1021/es60118a010
8. Furimsky E, Yumura M (1985) Solid adsorbents for removal of hydrogen sulphide from hot gas. doi: 10.4095/302594
9. Vamvuka D, Arvanitidis C, Zachariadis D (2004) Flue Gas Desulfurization at High Temperatures: A Review. Environmental Engineering Science 21(4): 525–548. doi: 10.1089/1092875041358557
10. Stemmler M, Tamburro A, Müller M (2013) Laboratory investigations on chemical hot gas cleaning of inorganic trace elements for the “UNIQUE” process. Fuel 108: 31–36. doi: 10.1016/j.fuel.2011.05.027
11. Focht GD, Ranade PV, Harrison DP (1988) High-temperature desulfurization using zinc ferrite: Reduction and sulfidation kinetics. Chemical Engineering Science 43(11): 3005–3013. doi: 10.1016/0009-2509(88)80053-8

12. Diego LFd, García-Labiano F, Adánez J et al. (1999) Factors Affecting the H 2 S Reaction with Noncalcined Limestones and Half-Calcined Dolomites. Energy Fuels 13(1): 146–153. doi: 10.1021/ef980145f
13. Katalambula H, Bawagan A, Takeda S (2001) Mineral attachment to calcium-based sorbent particles during in situ desulfurization in coal gasification processes. Fuel Processing Technology 73(2): 75–93. doi: 10.1016/S0378-3820(01)00200-4
14. Akiti T, Constant K, Doraiswamy L et al. (2001) Development of an advanced calcium-based sorbent for desulfurizing hot coal gas. Advances in Environmental Research 5(1): 31–38. doi: 10.1016/S1093-0191(00)00039-3
15. Katalambula H, Escallón MM, Takeda S (2001) Influence of Ca-Based Sorbent Particle Size on the Occurrence of Solid−Solid Reactions during in-Situ Desulfurization of the Coal-Derived Gas. Energy Fuels 15(2): 317–323. doi: 10.1021/ef000162g
16. Hartman M, Svoboda K, Trnka O et al. (2002) Reaction between Hydrogen Sulfide and Limestone Calcines. Ind. Eng. Chem. Res. 41(10): 2392–2398. doi: 10.1021/ie010805v
17. Álvarez-Rodríguez R, Clemente-Jul C (2008) Hot gas desulphurisation with dolomite sorbent in coal gasification. Fuel 87(17-18): 3513–3521. doi: 10.1016/j.fuel.2008.07.010
18. Sotirchos SV, Smith AR (2004) Performance of Porous CaO obtained from the decomposition of calcium-enriched bio-oil as Sorbent for SO_2 and H_2S Removal. Ind. Eng. Chem. Res. 43(6): 1340–1348. doi: 10.1021/ie034176w
19. Stemmler M, Tamburro A, Müller M (2013) Thermodynamic modelling of fate and removal of alkali species and sour gases from biomass gasification for production of biofuels. Biomass Conv. Bioref. 3(3): 187–198. doi: 10.1007/s13399-013-0073-7
20. Zeng Y, Kaytakoglu S, Harrison D (2000) Reduced cerium oxide as an efficient and durable high temperature desulfurization sorbent. Chemical Engineering Science 55(21): 4893–4900. doi: 10.1016/S0009-2509(00)00117-2

21. Flytzani-Stephanopoulos M, Sakbodin M, Wang Z (2006) Regenerative adsorption and removal of H_2S from hot fuel gas streams by rare earth oxides. Science (New York, N.Y.) 312(5779): 1508–1510. doi: 10.1126/science.1125684
22. Marcantonio V, Bocci E, Ouweltjes JP et al. (2020) Evaluation of sorbents for high temperature removal of tars, hydrogen sulphide, hydrogen chloride and ammonia from biomass-derived syngas by using Aspen Plus. International Journal of Hydrogen Energy 45(11): 6651–6662. doi: 10.1016/j.ijhydene.2019.12.142
23. A. Hatunoglu, V. Marcantonio, E. Ciro et al. (2021) D.2.4. High temperature secondary sorbents selection for inorganic compounds removal and related lab scale fixed bed reactor performance. EU Blaze Project Report, L'Aquila
24. Han K, Li X, Qi J et al. (2021) Synergistic effect of additives and blend on sulfur retention, on release and ash fusibility during combustion of biomass briquettes. International Journal of Green Energy 18(2): 187–202. doi: 10.1080/15435075.2020.1847116
25. Gehrig M, Wöhler M, Pelz S et al. (2019) Kaolin as additive in wood pellet combustion with several mixtures of spruce and short-rotation-coppice willow and its influence on emissions and ashes. Fuel 235: 610–616. doi: 10.1016/j.fuel.2018.08.028
26. Punjak WA, Shadman F (1988) Aluminosilicate sorbents for control of alkali vapors during coal combustion and gasification. Energy Fuels 2(5): 702–708. doi: 10.1021/ef00011a017
27. Dou B, Shen W, Gao J et al. (2003) Adsorption of alkali metal vapor from high-temperature coal-derived gas by solid sorbents. Fuel Processing Technology 82(1): 51–60. doi: 10.1016/s0378-3820(03)00027-4
28. Uberoi M, Punjak WA, Shadman F (1990) The kinetics and mechanism of alkali removal from flue gases by solid sorbents. Progress in Energy and Combustion Science 16(4): 205–211. doi: 10.1016/0360-1285(90)90029-3

29. Zheng Y, Jensen PA, Jensen AD (2008) A kinetic study of gaseous potassium capture by coal minerals in a high temperature fixed-bed reactor. Fuel 87(15-16): 3304–3312. doi: 10.1016/j.fuel.2008.05.003
30. Riese T de, Eckert D, Hakim L et al. (2022) Modelling the Capture of Potassium by Solid Al-Si Particles at Pulverised Fuel Conditions. Fuel 328: 125321. doi: 10.1016/j.fuel.2022.125321
31. Fujita S, Suzuki K, Mori T et al. (2003) A New Technique to Remove Hydrogen Chloride Gas at High Temperature Using Hydrogrossular. Ind. Eng. Chem. Res. 42(5): 1023–1027. doi: 10.1021/ie020158n
32. Khaled KF, Abdel-Rehim SS, Sakr GB (2012) On the corrosion inhibition of iron in hydrochloric acid solutions, Part I: Electrochemical DC and AC studies. Arabian Journal of Chemistry 5(2): 213–218. doi: 10.1016/j.arabjc.2010.08.015
33. Verdone N, Filippis P de (2006) Reaction kinetics of hydrogen chloride with sodium carbonate. Chemical Engineering Science 61(22): 7487–7496. doi: 10.1016/j.ces.2006.08.023
34. Li Y, Wu Y, Gao J (2004) Study on a New Type of HCl-Removal Agent for High-Temperature Cleaning of Coal Gas. Ind. Eng. Chem. Res. 43(8): 1807–1811. doi: 10.1021/ie034217o
35. Chyang C-S, Han Y-L, Zhong Z-C (2009) Study of HCl Absorption by CaO at High Temperature. Energy & Fuels 23(8): 3948–3953. doi: 10.1021/ef900234p
36. Abbasian J, Wangerow JR, Hill AH (1993) Effect of HCl on sulfidation of calcium oxide. Chemical Engineering Science 48(15): 2689–2695. doi: 10.1016/0009-2509(93)80181-O
37. Fujita S, Suzuki K, Shibasaki Y et al. (2002) Synthesis of hydrogarnet from molten slag and its hydrogen chloride fixation performance at high temperature. J Mater Cycles Waste Manag 4(1): 70–76. doi: 10.1007/s10163-001-0059-6
38. Fujita S, Suzuki K, Ohkawa M et al. (2001) Reaction of Hydrogrossular with Hydrogen Chloride Gas at High Temperature. Chem. Mater. 13(8): 2523–2527. doi: 10.1021/cm000863r
39. Stemmler M, Müller M (2010) D.4.1. Report on sorbents for alkali and sour gas removal. EU GreenSyngas-Project Report, Jülich

40. Bale CW, Bélisle E, Chartrand P et al. (2016) FactSage thermochemical software and databases, 2010–2016. Calphad 54: 35–53. doi: 10.1016/j.calphad.2016.05.002
41. Yazhenskikh E, Jantzen T, Hack K et al. (2019) A new multipurpose thermodynamic database for oxide systems. Rasplavy(2): 116–124. doi: 10.1134/S0235010619010237
42. Kopsch M, Lebendig F, Yazhenskikh E et al. (2024) Effect of HTC and Water-Leaching of Low-Grade Biomasses on the Release Behavior of Inorganic Constituents in a Calcium Looping Gasification Process at 650 °C. Energy Fuels 38(17): 16504–16519. doi: 10.1021/acs.energyfuels.4c02833
43. Wolf KJ, Müller M, Hilpert K et al. (2004) Alkali Sorption in Second-Generation Pressurized Fluidized-Bed Combustion. Energy & Fuels 18(6): 1841–1850. doi: 10.1021/ef040009c
44. Escobar I, Müller M (2007) Alkali Removal at about 1400 °C for the Pressurized Pulverized Coal Combustion Combined Cycle. 2. Sorbents and Sorption Mechanisms. Energy & Fuels 21(2): 735–743. doi: 10.1021/ef0605145
45. Weber CM (2008) Untersuchungen zum Alkaliverhalten unter Oxycoal-Bedingungen. Fakultät für Maschinenwesen. RWTH Aachen University, PhD-Thesis. Schriften des Forschungszentrums Jülich : […], Reihe Energie & Umwelt, Bd. 24, Aachen
46. Wolf KJ (2003) Untersuchungen zur Freisetzung und Einbindung von Alkalimetallen bei der reduzierenden Druckwirbelschichtverbrennung. Fakultät für Maschinenwesen. RWTH Aachen University, PhD-Thesis, Aachen
47. van der Kemp W, Blok JG, van der Linde PR et al. (1994) Binary alkaline earth oxide mixtures: Estimation of the excess thermodynamic properties and calculation of the phase diagrams. Calphad 18(3): 255–267. doi: 10.1016/0364-5916(94)90032-9
48. Brauer G (ed) (1978) Handbuch der präparativen anorganischen Chemie. In drei Bänden, 3., umgearb. Aufl. Enke, Stuttgart

659 49. Mayernick AD, Li R, Dooley KM et al. (2011) Energetics and Mechanism for H_2S Adsorption by Ceria-
660 Lanthanide Mixed Oxides: Implications for the Desulfurization of Biomass Gasifier Effluents. J. Phys.
661 Chem. C 115(49): 24178–24188. doi: 10.1021/jp206827n
662 50. Mullins DR, McDonald TS (2007) Adsorption and reaction of hydrogen sulfide on thin-film cerium
663 oxide. Surface Science 601(21): 4931–4938. doi: 10.1016/j.susc.2007.08.007